Journal of Histochemistry & Cytochemistry 2018, Vol. 66(5) 367–375

DOI: 10.1369/0022155418756308
journals.sagepub.com/home/jhc
SAGE

Perineurial-like Cells and EMA Expression in the Suprachoroidal Region of the Human Eye

Andrea R. Gilbert, Patricia Chévez-Barrios, and Matthew D. Cykowski
Department of Pathology, UT Health San Antonio, San Antonio, Texas (ARG); Department of Pathology and Genomic Medicine (ARG, PC-B, MDC) and Department of Ophthalmology, Blanton Eye Institute (PC-B), Houston Methodist Hospital, Houston, Texas; and Departments of Pathology and Laboratory Medicine (PC-B, MDC) and Ophthalmology (PC-B), Weill Cornell Medicine, New York City, New York

Summary
The suprachoroidal region of the eye comprises vascular channels, melanocytes, and thin fibroblasts with elongated cytoplasm that are positioned directly adjacent to the densely collagenous sclera. Morphological similarities between these suprachoroidal fibroblasts and arachnoid cells and perineurial cells have been recognized, but whether these fibroblasts have a perineurial cell-like immunophenotype is not known. To further examine the relationship of these three cell types, we investigated the comparative expression of epithelial membrane antigen (EMA), the tight junction protein claudin-1, glucose transporter-1 (Glut-1), and CD34 in suprachoroidal fibroblasts, arachnoid of the optic nerve sheath, and perineurium of ciliary nerves in eight human eye specimens. Granular, diffuse, and cytoplasmic EMA expression was seen in suprachoroidal fibroblasts, but this was not contiguous with the similar pattern of EMA expression in adjacent perineurium and arachnoid. CD34 expression in suprachoroidal fibroblasts was also seen, similar to arachnoid and perineurium. Claudin-1 and Glut-1 were not consistently expressed in suprachoroidal fibroblasts, distinguishing them from perineurial cells in particular and suggesting that these fibroblasts do not arise directly from adjacent arachnoid or perineurium. Nonetheless, the overlapping morphology and protein expression suggest phenotypic similarities in these cells that protect and support adjacent retina, optic nerve, and peripheral nerve. (J Histochem Cytochem 66:367–375, 2018)

Keywords
arachnoid, CD34, choroid, claudin-1, EMA, eye, Glut-1, perineurium, retina, suprachoroidal region

Introduction

The choroid, a component of the uvea, is a highly vascular region of the eye, positioned between the retina and retinal pigment epithelium on one side and the collagenous sclera on the other. Included within the choroid is a suprachoroidal region containing thin vascular channels, elastic and collagen fibers, elongated melanocytes, and fibroblasts.[1,2] The suprachoroidal fibroblasts help to form a transitional layer between sclera and the outermost choroid and are morphologically distinct, having flattened nuclei and long tapering cytoplasm. These cells are thought to secrete components of the choroid extracellular matrix, and groups of similar cells are joined by junctional complexes.[3]

The lamellar arrangement of thin fibroblasts with elongated cytoplasm in the suprachoroidal region resembles the arrangement of cells in perineurium in particular. Studies performed nearly five decades ago even suggested that suprachoroidal fibroblasts had ultrastructural features similar to arachnoid and perineurium.[4,5] Based on these studies, it was hypothesized

Received for publication September 26, 2017; accepted January 2, 2018.

Corresponding Author:
Matthew D. Cykowski, Department of Pathology and Genomic Medicine, Houston Methodist Hospital, 6565 Fannin Street, Houston, TX, 77030, USA.
E-mail: mdcykowski@houstonmethodist.org

Journal of Histochemistry & Cytochemistry

Table 1. Antibodies Used in the Study.

Antibody	Vendor	Species	Clone	Dilution
EMA	CellMarque (Rocklin, CA)	Mouse monoclonal	E29	1:200
EMA	Ventana (Tucson, AZ)	Mouse monoclonal	E29	Predilute
Claudin-1	Invitrogen (Waltham, MA)	Rabbit polyclonal	NA	1:50
Glut-1	Sigma-Aldrich (St. Louis, MO)	Rabbit monoclonal	SP168	1:200
CD34	Ventana (Tucson, AZ)	Mouse monoclonal	QBEnd/10	Predilute

Abbreviation: EMA, epithelial membrane antigen.

that perineurial cells, arachnoid cells, and suprachoroidal fibroblasts might even share a common embryological origin or form a contiguous connective tissue sheath surrounding nerve, central nervous system, and retina.[5] Along similar lines, perineurium is thought by some to be an extension of the arachnoid along the nerve root,[6] which is reflected in their morphological and immunophenotypical similarities. This anatomic link may also reflect a shared functional significance as perineurial cells help to form the blood–nerve barrier,[6] and arachnoid cells help to form the brain–cerebrospinal fluid barrier.[7] If the arachnoid–perineurium link could be further extended to suprachoroidal fibroblasts in the eye, it might suggest that these specialized fibroblasts have an analogous role in protection of the eye and retina.

To further examine the potential relationship between suprachoroidal fibroblasts, perineurial cells, and arachnoid, we examined the extent to which suprachoroidal fibroblasts express proteins that have been well studied in the latter two cell types (arachnoid and perineurium). We hypothesized that the immunophenotype of these three cell types would be similar, if not identical, reflecting a common precursor in development or perhaps even direct anatomic continuity. To test this hypothesis, we examined the expression of epithelial membrane antigen (EMA), the tight junction protein claudin-1, glucose transporter-1 (Glut-1), and the transmembrane protein CD34 in eight adult human eye specimens, comparing the pattern of expression in suprachoroidal fibroblasts, arachnoid cells of the optic nerve sheath, and perineurium of the ciliary nerves.

Materials and Methods

Identification of Tissues for Histological Study

The study sample included the enucleation specimens of patients treated at our institution for uveal melanoma. The typical specimen examined contained a section through optic nerve, dura and leptomeninges, sclera and periocular soft tissue, ciliary nerves, retina and choroid, ciliary body, iris, and cornea. This sample type was specifically chosen as it afforded us the opportunity to study the structures of interest in areas of the eye uninvolved by tumor and in patients without other end-stage ocular pathologies. Samples were included only if they contained relatively small uveal melanomas with intact choroid that was not replaced by tumor. Exclusion criteria included the (1) absence of choroid in the section, (2) choroid that was largely involved by tumor, and (3) choroid that was disrupted such that normal architecture could not be appreciated. Controls were not available as a comparison group. However, to confirm the immunoreactivity identified in the uveal melanoma specimens, an additional eye without tumor was submitted for immunohistochemical staining. This specimen was the uninvolved eye of a patient with uveal melanoma who came to autopsy at our institution. One of the authors (P.C.-B.), an ophthalmic pathologist, reviewed the specimens, confirmed the pathological diagnoses, and assessed the intactness of the uninvolved choroid. Demographic and clinical data were identified in the medical record as appropriate, and the study was carried out with the approval of the Institutional Review Board at Houston Methodist Hospital.

Histological and Immunohistochemical Procedures

At the time of enucleation, the fresh specimens were fixed in 10% buffered formalin within 1 hr. Tissue was sampled, blocked, and processed after a period of fixation not exceeding 2 weeks. Formalin-fixed, paraffin-embedded tissue was then sectioned at 5 µm, mounted on positively charged slides, and dried at 60C. H&E staining was performed using an automated stainer in our laboratory.

Antibodies applied to all specimens are listed in Table 1, including antibody name, vendor, antibody dilution, and clone (catalog number for claudin-1 is 71-7800). For two of these antibodies (Ventana predilute EMA and CD34), automated immunostaining at our institution was performed using the BenchMark

ULTRA platform (Ventana Medical Systems, Inc.; Tucson, AZ). Appropriate positive and negative controls were performed with both antibodies.

For the remaining three antibodies (CellMarque EMA, Glut-1, and claudin-1), staining was performed in the laboratory of one of the study authors (M.D.C.) after establishing appropriate dilutions of each. Each staining experiment was performed with negative controls and sections of tonsil as a positive control. For each antibody, sections were deparaffinized and rehydrated through a series of alcohols and water. Heat-based antigen retrieval was performed using a 1× antigen retrieval solution at pH 9 (Agilent Technologies; Santa Clara, CA) carried out for 1 hr (30 min at 95C followed by 30 min on ice). All washing steps were carried out using a commercial Tris-buffered saline solution (1×) containing Tween 20, pH 7.6 (Agilent Technologies). A 3% hydrogen peroxide solution (VWR International; Radnor, PA) was used to block endogenous peroxidase. Primary antibody was applied overnight at 4C following a 1-hr blocking step at room temperature with 2.5% horse serum (Vector Laboratories; Burlingame, CA). Slides were thoroughly washed and the ImmPress horseradish peroxidase (HRP) anti-rabbit and anti-mouse IgG detection kits (Vector Laboratories) were applied as appropriate for 1 hr at room temperature. Following additional washing steps, target antigen was visualized using DAB chromogen in substrate buffer (Agilent Technologies). After additional washing steps, hematoxylin counterstain was applied, and slides were brought to xylene and mounted with Permount (ThermoFisher Scientific; Waltham, MA).

Immunofluorescence Procedures

Immunofluorescence preparations were also made, including preparations using monoclonal CellMarque EMA as well as double labeling with CellMarque EMA and the neuronal marker MAP-2 (rabbit polyclonal, 1:100, 17490-1-AP, Proteintech; Rosemont, IL). The latter was performed to highlight the relationship of EMA-positive cells to the remainder of choroid, retinal pigment epithelium, and retina. Briefly, slides were incubated overnight with primary antibody at 4C following deparaffinization, rehydration, and antigen retrieval procedures (as above) and a blocking step using 2.5% horse serum. After several washes with fresh phosphate-buffered saline, secondary antibodies were applied for 1 hr at room temperature, including Alexa Fluor 555 Anti-Rabbit IgG (1:200; A21429), Alexa Fluor 555 Anti-Mouse IgG (1:200; A32727), Alexa Fluor 488 anti-Mouse IgG (1:200; A11001), and Alexa Fluor 488 anti-Rabbit IgG (1:200; A11034) (Alexa Fluor products of ThermoFisher), as appropriate. For double-labeling staining experiments, appropriate dilutions of combined primary and secondary antibodies were made in 2.5% horse serum and applied to the slide simultaneously at those steps in the protocol. After additional washing steps, slides were mounted using Vectashield Antifade mounting medium with 4′,6-diamidino-2-phenylindole (DAPI; Vector Laboratories). These slides were reviewed within 24 hr of staining, and images were captured in cellSens software 1.13 (Olympus America, Inc.; Center Valley, PA) on an Olympus BX-43 Microscope using a DP71 camera, an enhanced green fluorescent protein (EGFP) FITC/Cy2 filter cube (set number 49002, Olympus; Center Valley, PA), and a CY3/tetramethylrhodamine-isothiocyanate (TRITC) filter cube (set number 49004, Olympus). Slides were examined separately under DAPI, TRITC, and FITC filters, captured, and merged in cellSens.

Qualitative and Semi-quantitative Assessment of Staining in Specimens

Two pathologists (A.G., P.C.-B.) performed qualitative and semi-quantitative rating on each sample. Extent of staining, staining intensity, and region of choroid with immunoreactive foci were each assessed as described below and agreed upon by both of these authors. The third author (M.D.C.), also a pathologist, separately reviewed those evaluations and slide materials and concurred. Extent of immunostaining for each ocular structure was designated as either focal (F) or diffuse (D). Staining intensity in optic nerve sheath arachnoid cells, perineurial cells of the ciliary nerves, and suprachoroidal fibroblasts was also assessed. Intensity of staining was assigned a value based on a 4-point scale: +++ (strong), ++ (moderate), + (weak), and – (none). Labeling of suprachoroidal fibroblasts was also assessed in three regions of choroid: the posterior pole (near the optic nerve disc), the anterior pole (near the ora serrata), and the equator, equidistant between the anterior and posterior poles.

Results

Demographic and Clinical Characteristics

Eight specimens were selected (four left, four right) that met inclusion criteria as described above. The enucleation specimens were from three men and five women, ranging from 23 to 94 years in age (median age, 69.5 years; first quartile, 61.8 years; third quartile, 80.8 years). All enucleation specimens contained uveal melanoma with variable involvement of choroid (focal, not extensive), ciliary body, and/or iris. Additional

Table 2. Patient Demographics, Specimen Type, and Specimen Diagnoses.

Case	Age (Years)	Sex	Sample	Primary Diagnosis	Additional Diagnoses
1	52	F	R eye	UM involving choroid, CB, iris	Treatment effect, CR scars, epiretinal membranes, ON atrophy
2	73	M	L eye	UM involving choroid, CB	Vitreous hemorrhage, PP, ON atrophy
3	79	F	R eye	UM involving CB, iris	Retinal PCD, vitreous asteroid hyalosis
4	94	F	L eye	UM involving choroid, CB, iris	Macular edema, retinal PCD, PP
5	23	F	L eye	UM involving choroid, CB, iris	RD
6	65	F	R eye	UM involving choroid, CB, iris	RD, ON atrophy
7	66	M	L eye	UM involving choroid, CB	RD, ON atrophy, PP
8	86	M	R eye	UM involving choroid	Macular edema, ON atrophy, PP

Abbreviations: F, female; R, right; UM, uveal melanoma; CB, ciliary body; CR, chorioretinal; ON, optic nerve; M, male; L, left; PP, pseudophakia; PCD, peripheral cystic degeneration; RD, retinal detachment.

pathologies commonly identified included mild optic nerve atrophy, peripheral cystic degeneration of the retina, retinal detachment, and pseudophakia. Complete demographic data, specimen type, and diagnoses are listed for each of the eight specimens in Table 2. As described above, an additional right eye specimen was also examined from a patient coming to autopsy who had a history of uveal melanoma in the left eye. The uninvolved right eye, examined by one of the study authors (P.C.-B.), an ophthalmic pathologist, was grossly unremarkable. Microscopic examination of this eye revealed non-neoplastic pathologies, including peripheral cystoid retinal degeneration, and the specimen was negative for melanoma, including within the vortex veins.

Immunohistochemical Results

Figure 1 depicts the pattern of staining for EMA (both antibodies), Glut-1, and claudin-1 in perineurium (top row), arachnoid (middle row), and suprachoroidal fibroblasts (bottom row), respectively. The results of immunohistochemistry for EMA (Ventana and CellMarque antibodies), CD34, claudin-1, and Glut-1 protein expression within optic nerve sheath arachnoid cells, ciliary nerve perineurial cells, and suprachoroidal fibroblasts are also listed in Table 3.

As shown in Table 3, EMA labeled suprachoroidal fibroblasts (100% of specimens with both CellMarque and Ventana antibodies), arachnoid cells (100%), and perineurium (100% with CellMarque EMA and all but one sample with Ventana EMA). One sample had technical issues that were not resolved upon repeating the Ventana EMA stain (using the automated procedure as described above), but this specimen was positive with the CellMarque antibody. As shown in Fig. 2, despite diffuse labeling of the cells, suprachoroidal fibroblasts demonstrated some regional variation in EMA staining intensity, which was greatest at the equator and anterior pole of the eye. No continuity between EMA-reactive suprachoroidal fibroblasts and either arachnoid (at the posterior pole) or perineurial cells (entering the eye with the ciliary nerves) was identified.

CD34 also labeled suprachoroidal fibroblasts in all specimens (100%), as shown in Table 3. CD34 labeling was diffuse in these cells in six specimens and focal in two. Furthermore, 100% of specimens had immunoreactivity for CD34 in arachnoid cells of optic nerve sheath and in 75% of specimens within perineurial cells. Strong and diffuse perineurial staining for CD34 was identified in five specimens while one specimen had moderate intensity, diffuse staining. Figure 2 shows that CD34 staining intensity in suprachoroidal fibroblasts was fairly consistent within specimens from posterior pole to equator to anterior pole.

Diffuse, moderate-to-strong claudin-1 labeling was seen in only 25% of specimens within suprachoroidal fibroblasts. The remaining samples had weak or focal staining (37.5%) (Table 3, Fig. 2) or were entirely negative for claudin-1 (37.5%). Within arachnoid, claudin-1 was positive in six specimens (75%), showing moderately intense staining in 4 specimens and weak staining in two. Claudin-1 labeling was most reliable within perineurial cells, being present in 87.5% of specimens and of moderate or strong intensity in 62.5% of specimens.

As with claudin-1, Glut-1 was not a reliable marker of suprachoroidal fibroblasts. Glut-1 was completely negative in 62.5% of specimens within suprachoroidal fibroblasts, and staining was only focal in two of the three immunoreactive specimens. In contrast, Glut-1 demonstrated diffuse, moderate-to-strong intensity staining of perineurial cells in all specimens (100%) and was positive in 75% of specimens within arachnoid.

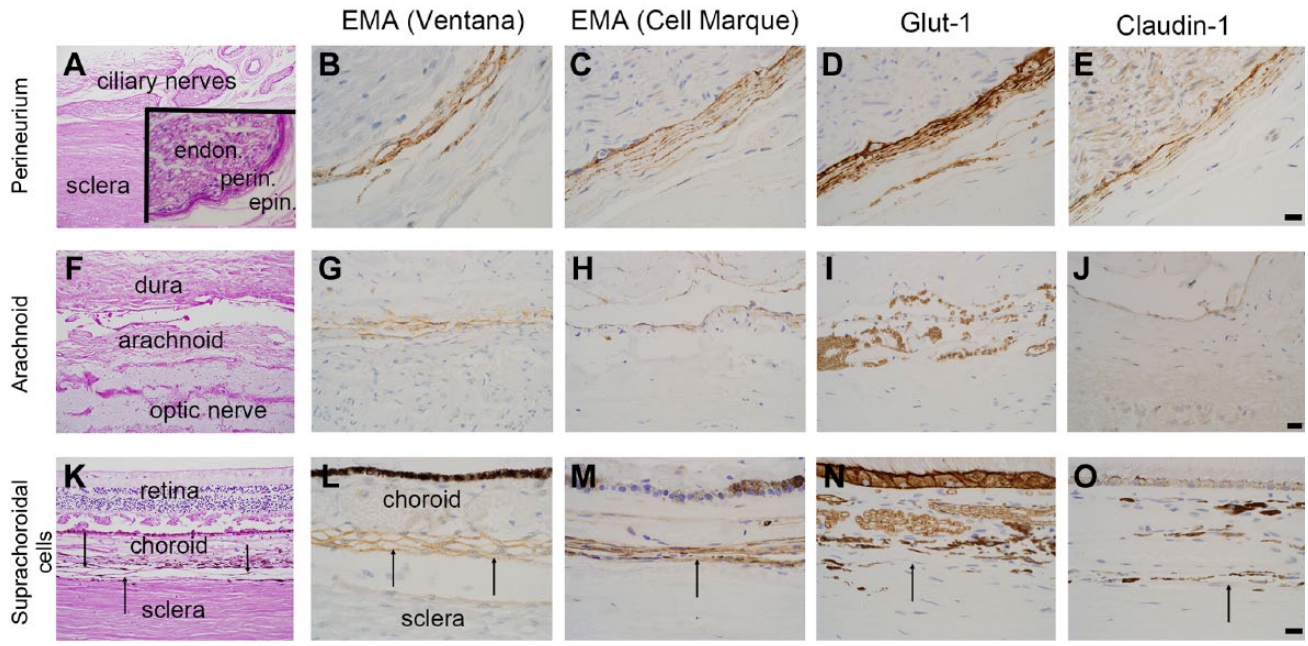

Figure 1. Immunophenotype of perineurial cells, arachnoid, and suprachoroidal cells. Immunohistochemical profile of perineurial cells (panels A–E), optic nerve sheath/arachnoid (F–J), and suprachoroidal cells (K–O, indicated by black arrows). Panel A shows ciliary nerves and sclera of the posterior eye with an inset showing endoneurium (endon.), perineurium (perin.), and epineurium (epin.) of a ciliary nerve. Perineurial cells are immunoreactive for 2 EMA antibodies (B, C), Glut-1 (D), and claudin-1 (E). Panel F shows optic nerve sheath with arachnoid, which is immunoreactive for both EMA antibodies (G, H), weakly reactive for claudin-1 (J), and negative for Glut-1 (I). Panel K shows retina, choroid, thin suprachoroidal cells, and sclera. Suprachoroidal cells, indicated by black arrows, are immunoreactive for EMA (L, M), and, in these examples, immunonegative for Glut-1 (N) and claudin-1 (O). Examples are from multiple samples with panels B–E and L–O at 600× (panel E, O scale bars = 20 μm) and panels G–J at 400× (panel J scale bar = 20 μm). Lower-power, PAS-stained images (A, F, K) at 100×. Abbreviations: EMA, epithelial membrane antigen; PAS, periodic acid–Schiff.

Table 3. Immunostaining Results in Suprachoroidal Fibroblast-like, Perineurium, and Arachnoid.

	EMA (CellMarque)			EMA (Ventana)			CD34			Claudin-1			Glut-1		
Specimen	AC	PC	FLC	AC	PC	FLC	AC	PC	FLC	AC	PC	FLC	AC	PC	FLC
1	+++D	+++D	+++D	+++D	–	++D	+++D	–	++D	–	–	+++D	–	+++D	–
2	+++D	+++D	+++D	+++D	+++D	+++D	+++D	–	+++D	+D	+++D	+D	+++D	+++D	+F
3	+++D	+D	+++D	NaN	NaN	NaN	+++D	+++D	+F	+D	++D	–	++D	++D	–
4	+++D	+++D	+++D	+++D	++D	+++D	++D	++D	+F	++D	++D	++D	+D	+++D	–
5	+++D	++D	+++D	++D	+F	+D	+++F	+++D	+++D	–	+D	+D	–	+++D	++F
6	+++D	++D	++D	+++D	+++F	++D	++F	+++D	+++D	++D	++D	–	++F	++D	–
7	+++D	++D	+++D	+++D	+F	++D	+++D	+++D	+++D	++F	+F	+F	++D	+++D	++D
8	+++D	++D	+++D	+++F	++D	+++D	+++F	+++D	++D	++D	++D	–	+++D	+++D	–

Staining intensity is represented by the symbols above as follows: +++ = strong, ++ = moderate, + = weak, and – = negative. Extent of staining is represented by the letters above as either "D" (diffuse) or "F" (focal). Each of the eight cases is represented by a single row. Abbreviations: EMA, epithelial membrane antigen; AC, arachnoid cells; PC, perineurial cells; FLC, suprachoroidal fibroblast-like cell.

Control eyes were not available for comparison, but examination of an eye uninvolved by tumor revealed a similar pattern of staining with both EMA antibodies and no labeling of suprachoroidal fibroblasts by Glut-1 or claudin-1 (please see Supplemental Fig. 1). For EMA, the same pattern of granular, cytoplasmic immunoreactivity was identified as in the study specimens involved by uveal melanoma.

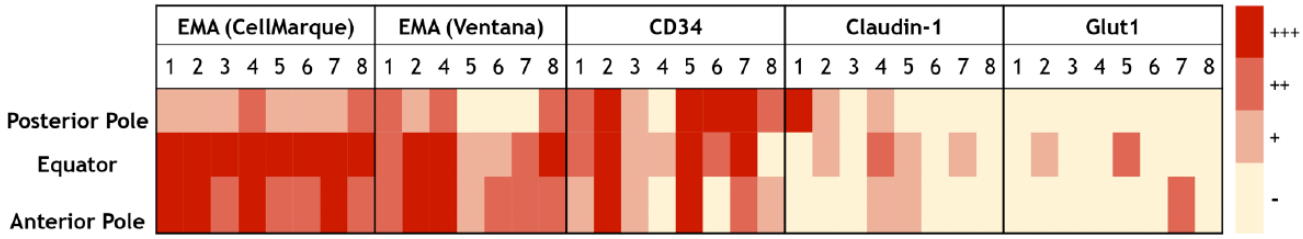

Figure 2. A heat map of staining intensity of suprachoroidal fibroblasts for EMA antibodies (CellMarque, Ventana), CD34, claudin-1, and Glut-1 in the posterior pole, equator, and anterior pole of the eye. Each antibody has specimens 1–8 listed in columns with anatomic region of interest listed in rows. A scale for staining intensity is present at the right of the figure. Abbreviation: EMA, epithelial membrane antigen.

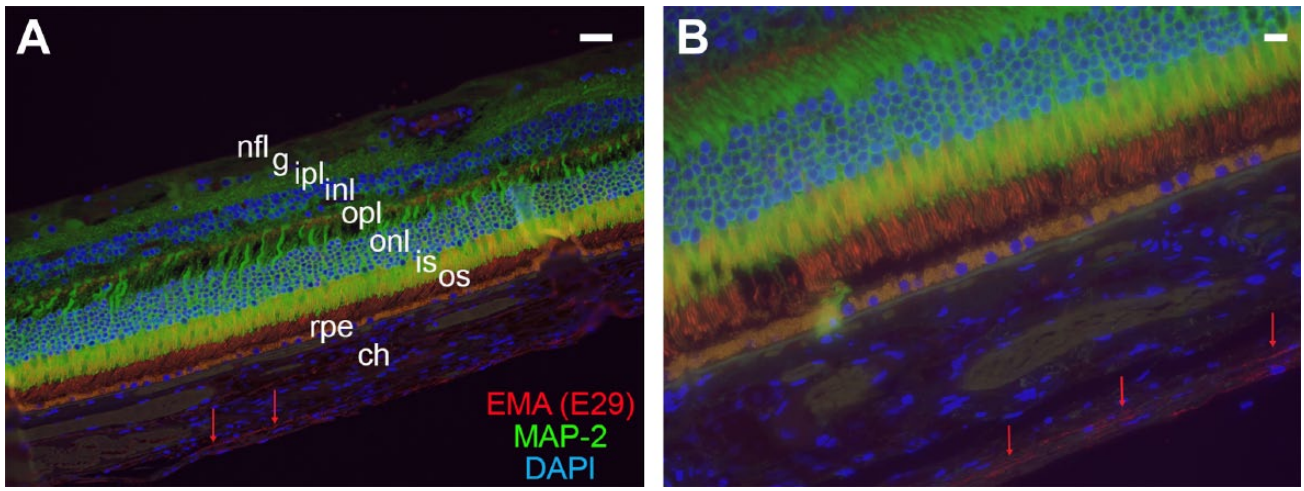

Figure 3. Relationship of suprachoroidal fibroblasts to choroid and retina. Immunofluorescence preparations of retina, choroid, and suprachoroidal cells with double labeling for EMA (clone E29) (TRITC), the neuronal marker MAP-2 (FITC), and DAPI (FITC/TRITC/DAPI merged images). The EMA-immunoreactive cells are indicated by the red arrows in both images and comprise elongated, thin fibroblasts or fibroblast-like cells between choroid and sclera (not shown). Layers of retina shown include the nerve fiber layer (nfl), ganglion cell layer (g), inner plexiform layer (ipl), inner nuclear layer (inl), outer plexiform layer (opl), outer nuclear layer (onl), and inner (is) and outer segments (os) of the photoreceptor layer. Retinal pigment epithelium (rpe) is the yellow-orange layer deep to retina and demonstrates yellow-orange, autofluorescent signal in the merged image. Images are taken at 400× (A) and 600× (B) with both scale bars (upper right-hand corner of both images) representing 20 µm. Abbreviations: EMA, epithelial membrane antigen; TRITC, tetramethylrhodamine-isothiocyanate; DAPI, 4′,6-diamidino-2-phenylindole; MAP-2, microtubule-associated protein 2.

Immunofluorescence Results

To evaluate the relationship of suprachoroidal fibroblasts to retina, retinal pigment epithelium, and sclera, double-labeling immunofluorescence studies were carried out with MAP-2 (to mark retinal neurons) and EMA (to mark suprachoroidal fibroblasts). As shown in merged image of Fig. 3 (DAPI/TRITC/FITC), EMA labeling (red/TRITC filter) was identified in elongated, thin cells of the suprachoroidal layer. Examination of the cells under the FITC/Cy2 filter revealed no autofluorescent signal (in contrast, autofluorescence was seen in retinal pigment epithelium, as seen in Fig. 3, panel A). Additional examples of the morphology and single antibody immunofluorescence labeling for EMA are shown in Fig. 4A, Fig. 4B (perineurium), and Fig. 4C, 4D (suprachoroidal fibroblasts). As in Fig. 3, Fig. 4B and Fig. 4D are merged DAPI/FITC/TRITC images.

Discussion

The morphological similarities of suprachoroidal fibroblasts, arachnoid cells, and perineurial cells were previously described by ultrastructural examination, and it has been suggested that the fibroblasts within choroid, perineurium, and arachnoid of the nervous system are ultrastructurally and histochemically identical.[5] Our findings extend the similarities to the immunophenotype of each of these three cell types. In particular, immunoreactivity for EMA and CD34 was seen in suprachoroidal fibroblasts, and this closely paralleled the reactivity observed in adjacent perineurial cells

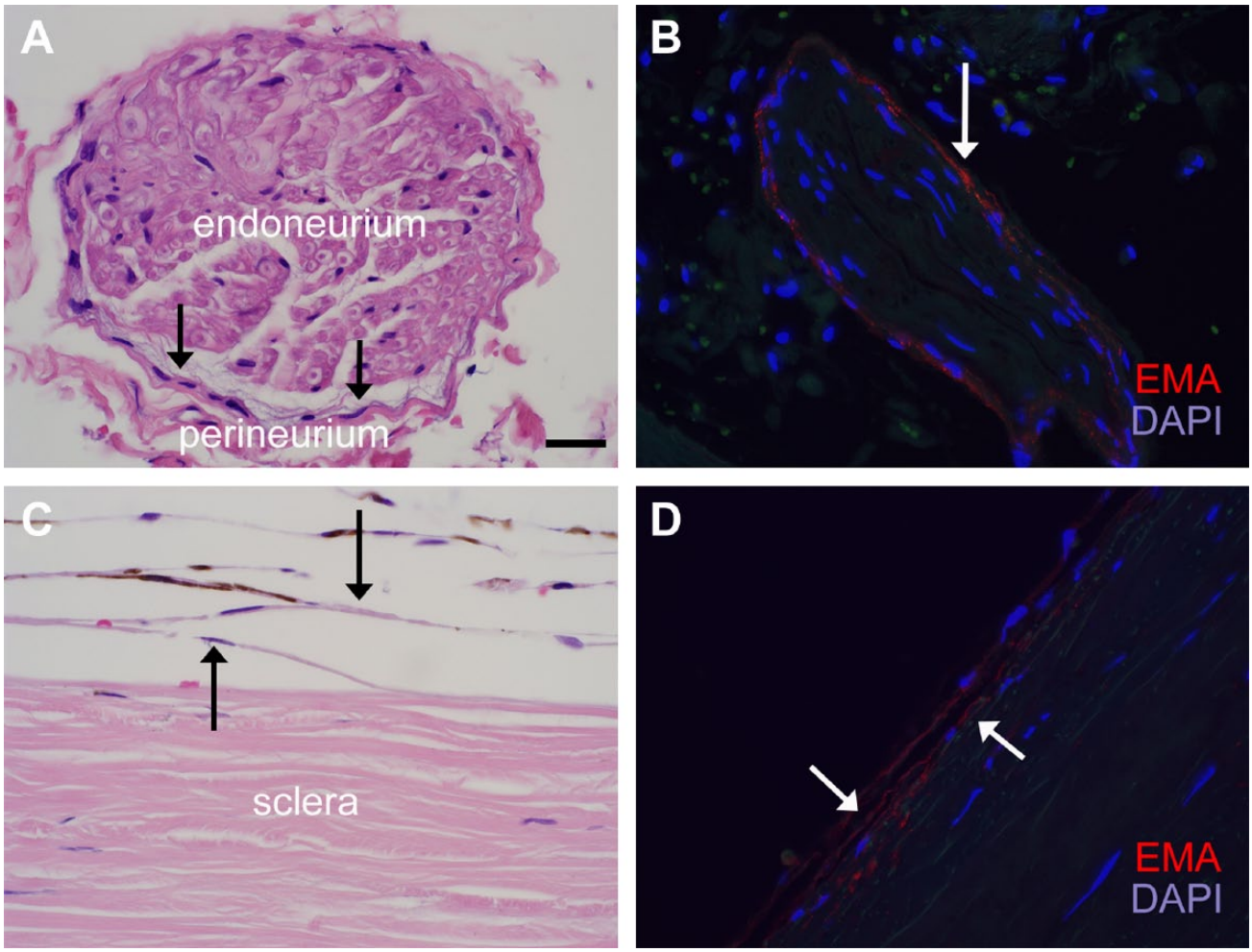

Figure 4. Similarities in the morphology and EMA reactivity of perineurial and suprachoroidal cells. H&E images (panels A and C) and immunofluorescence for EMA (E29) (panels B and D) highlight the morphological and immunohistochemical similarities of the perineurium of small ciliary nerves (A, B) and suprachoroidal cells between choroid and sclera (C, D). Both cell groups, indicated by black arrows in panels A and C, respectively, comprise thin fibroblasts with long cytoplasmic processes and flattened nuclei. Melanin pigment is also seen in melanocytes of this suprachoroidal region. EMA (E29) (TRITC) shows a similar pattern of granular, cytoplasmic immunoreactivity in both cell types (see also Fig. 1). Images are taken at 600× (scale bars in panel A = 20 μm). Abbreviations: EMA, epithelial membrane antigen; TRITC, tetramethylrhodamine-isothiocyanate; DAPI, 4′,6-diamidino-2-phenylindole.

and arachnoid cells. However, the immunoprofile of adjacent perineurial cells of ciliary nerves in particular (EMA+/CD34+/claudin-1+/Glut-1+) was not fully recapitulated in the suprachoroidal fibroblasts in the majority of specimens. Likewise, although direct continuity between pia-arachnoid and choroid has been suggested,[5] we did not observe direct continuity of immunoreactive suprachoroidal fibroblasts and arachnoid cells of the nerve sheath adjacent to the lamina cribrosa. From our findings, and those of earlier studies, we conclude that suprachoroidal fibroblasts may be a distinct cell with perineurial cell-like qualities morphologically and, to some extent, in their immunohistochemical profile. We also conclude that suprachoroidal fibroblasts do not have an identical immunophenotype to, and may not be directly contiguous with, the perineurium of the ciliary nerves or arachnoid of the optic nerve sheath.

The choroid is a vascular structure thought to support the retina through a variety of homeostatic functions, as well as providing the major source of blood supply to the outer retina.[3] The suprachoroidal fibroblasts studied here are located in the outermost lamina of choroid (also known as the lamina fusca or suprachoroidea).[1,3] Similar to leptomeningeal arachnoid cells and perineurial cells of the nerve sheath, these fibroblasts are characterized by elongated and interdigitating cytoplasmic processes, cytoplasmic vesicles, and junctional complexes.[3,8–13] As such, these fibroblast or fibroblast-like cells may have a

unique protective or supportive function for the overlying retina, reflected by a unique morphology and immunoprofile. Here, we identified a very similar expression pattern of granular, cytoplasmic EMA expression in suprachoroidal fibroblasts, arachnoid cells, and perineurial cells (Figs. 1 and 4). Although it is well known that EMA is expressed in normal arachnoid cells and meningioma,[14–16] as well as in perineurial cells[17,18] and perineurioma,[19] to our knowledge, this is the first demonstration of similar staining in suprachoroidal fibroblasts. We also identified regional differences in EMA expression in the choroid, with generally greater EMA intensity at the equator and anterior pole (Fig. 2). This initially raised the question as to whether the suprachoroidal fibroblasts in choroid were contiguous with perineurium of ciliary nerves entering the eye, hence the greater intensity in more anterior regions as the small nerves traverse the sclera and pass into choroid accompanied by their thin perineurium. However, within the same specimens, the frequent lack of claudin-1 and particularly Glut-1 expression, both of which highlighted perineurium, argues against that possibility. As such, the reason(s) for greater intensity of EMA expression in the choroid of equator and anterior pole are not known. CD34, a transmembrane glycoprotein of fibroblastic mesenchymal cells,[20,21] also labeled the EMA-reactive suprachoroidal cells, further suggesting that these cells indeed represent some type of modified fibroblast. Immunoreactivity for CD34 was also seen in all specimens within arachnoid cells and, in the majority of samples, within normal perineurium.

In contrast to EMA and CD34, Glut-1 and claudin-1 were not reliable markers of suprachoroidal fibroblasts, despite their perineurial cell-like qualities. Claudin-1 is a transmembrane protein that is an integral component of tight junctions, but in our specimens, it showed predominantly weak or entirely absent labeling of suprachoroidal fibroblasts. Claudin-1 is known to label arachnoid cells, which contain complex tight junctions that form a meshwork, accompanied by desmosomes and gap junctions.[10] In perineurial cells, claudin-1 likewise showed a strong, particulate pattern of membranous staining[22] that probably reflects the presence of tight junctions.[17] In suprachoroidal fibroblasts, the inconsistent result with claudin-1 was surprising, as these cells are also reported to have junctional complexes, including adherens and occluding junctions.[3] Additional markers may be useful in better highlighting the junctional complexes of these suprachoroidal fibroblasts (e.g., occludin, ZO-1, and claudin-4). The absence of Glut-1 labeling in the suprachoroidal fibroblasts in the majority of specimens provided an even stronger distinction between suprachoroidal fibroblasts and adjacent perineurial cells. Glut-1 labels the most common isoform of a glucose transporter and is typically expressed in perineurium,[6,23,24] but it is not tissue-specific and is expressed in many cell types (endothelium, epithelium, red blood cells).[25] Additional markers of perineurial cells, including collagen IV[22] and laminin, may also be worth investigating in future studies of suprachoroidal fibroblasts.

In summary, we compared the immunoprofile of three cell types in the eye with very similar morphological and ultrastructural features, each likely representing a type of modified fibroblast or mesenchymal cell (arachnoid cell, perineurial cell, and suprachoroidal fibroblasts). The most consistent immunoprofile seen in the suprachoroidal cells—positive for EMA and CD34 and negative or equivocal for claudin-1 and Glut-1—overlapped to some extent, but not completely, with the profile of normal arachnoid and perineurium in the same specimens. Although these suprachoroidal fibroblasts may have a supportive or protective role, similar to arachnoid and perineurial cells, our findings argue against these three cell types constituting a single, contiguous covering or even being in direct continuity with each other. Rather, modified fibroblasts in various anatomic sites within and adjacent to the eye (choroid, arachnoid, and perineurium) may have similar morphological, ultrastructural, and immunohistochemical features that reflect their protective and supportive functions. A limitation of this study is that it only included human eyes, and the majority of these were diseased due to the nature of specimens received at our institution. Whether the immunoprofile of suprachoroidal fibroblasts is similar in animal eyes, including those of non-human primates, is also not known. Further studies are required to understand the potentially unique function(s) of suprachoroidal fibroblast, as this may provide insight into the various diseases of the eye that involve the choroid.

Acknowledgments

We are grateful for the excellent technical assistance provided by the personnel of the histology and immunohistochemistry sections in the Department of Pathology and Genomic Medicine at Houston Methodist Hospital.

Competing Interests

The author(s) declared no potential conflicts of interest with respect to the research, authorship, and/or publication of this article.

Author Contributions

All three authors contributed substantially to the article as follows: ARG collected data, performed analyses, and drafted the initial version of the manuscript; PC-B helped to

design the study, provided expert ophthalmological pathology interpretation of slides, and assisted ARG in data analysis; PC-B also reviewed and critically revised the manuscript; MDC help to design the study, performed several of the staining experiments described herein, reviewed the data, and reviewed and critically revised the manuscript. All authors approve the final version as submitted.

Funding

The author(s) disclosed receipt of the following financial support for the research, authorship, and/or publication of this article: This work was supported in part by a Clinician-Scientist Research Award from the Institute of Academic Medicine in the Houston Methodist Research Institute (HMRI) of the Houston Methodist Hospital (to M.D.C.).

Literature Cited

1. Feeney L, Hogan MJ. Electron microscopy of the human choroid. I. Cells and supporting structure. Am J Ophthalmol. 1961;51:1057–72.
2. Hogan MJ. Ultrastructure of the choroid. Its role in the pathogenesis of chorioretinal disease. Trans Pac Coast Otoophthalmol Soc Annu Meet. 1961;42:61–87.
3. Nickla DL, Wallman J. The multifunctional choroid. Prog Retin Eye Res. 2010;29(2):144–68. doi:10.1016/j.preteyeres.2009.12.002.
4. Shanthaveerappa TR, Bourne GH. The perineural epithelium of sympathetic nerves and ganglia and its relation to the pia arachnoid of the central nervous system and perineural epithelium of the peripheral nervous system. Z Zellforsch Mikrosk Anat. 1964;61:742–53.
5. Shanthaveerappa TR, Bourne GH. Histological and histochemical studies of the choroid of the eye and its relations to the pia-arachnoid mater of the central nervous system and perineural epithelium of the peripheral nervous system. Acta Anat (Basel). 1965;61(3):379–98.
6. Pina-Oviedo S, Ortiz-Hidalgo C. The normal and neoplastic perineurium: a review. Adv Anat Pathol. 2008;15(3):147–64.doi:10.1097/PAP.0b013e31816f8519.
7. Vandenabeele F, Creemers J, Lambrichts I. Ultrastructure of the human spinal arachnoid mater and dura mater. J Anat. 1996;189(Pt 2):417–30.
8. Erlandson RA, Woodruff JM. Peripheral nerve sheath tumors: an electron microscopic study of 43 cases. Cancer. 1982;49(2):273–87.
9. Giannini C, Scheithauer BW, Jenkins RB, Erlandson RA, Perry A, Borell TJ, Hoda RS, Woodruff JM. Soft-tissue perineurioma. Evidence for an abnormality of chromosome 22, criteria for diagnosis, and review of the literature. Am J Surg Pathol. 1997;21(2):164–73.
10. Hasegawa M, Yamashima T, Kida S, Yamashita J. Membranous ultrastructure of human arachnoid cells. J Neuropathol Exp Neurol. 1997;56(11):1217–27.
11. Kida S, Yamashima T, Kubota T, Ito H, Yamamoto S. A light and electron microscopic and immunohistochemical study of human arachnoid villi. J Neurosurg. 1988;69(3):429–35. doi:10.3171/jns.1988.69.3.0429.
12. Shanthaveerappa TR, Bourne GH. A perineural epithelium. J Cell Biol. 1962;14:343–6.
13. Yamashima T, Kida S, Yamamoto S. Ultrastructural comparison of arachnoid villi and meningiomas in man. Mod Pathol. 1988;1(3):224–34.
14. Theaker JM, Gatter KC, Esiri MM, Fleming KA. Epithelial membrane antigen and cytokeratin expression by meningiomas: an immunohistological study. J Clin Pathol. 1986;39(4):435–9.
15. Theaker JM, Gillett MB, Fleming KA, Gatter KC. Epithelial membrane antigen expression by meningiomas, and the perineurium of peripheral nerve. Arch Pathol Lab Med. 1987;111(5):409.
16. Meis JM, Ordonez NG, Bruner JM. Meningiomas. An immunohistochemical study of 50 cases. Arch Pathol Lab Med. 1986;110(10):934–7.
17. Ariza A, Bilbao JM, Rosai J. Immunohistochemical detection of epithelial membrane antigen in normal perineurial cells and perineurioma. Am J Surg Pathol. 1988;12(9):678–83.
18. Perentes E, Nakagawa Y, Ross GW, Stanton C, Rubinstein LJ. Expression of epithelial membrane antigen in perineurial cells and their derivatives. An immunohistochemical study with multiple markers. Acta Neuropathol. 1987;75(2):160–5.
19. Hornick JL, Fletcher CD. Soft tissue perineurioma: clinicopathologic analysis of 81 cases including those with atypical histologic features. Am J Surg Pathol. 2005;29(7):845–58.
20. Chaubal A, Paetau A, Zoltick P, Miettinen M. CD34 immunoreactivity in nervous system tumors. Acta Neuropathol. 1994;88(5):454–8.
21. Cummings TJ, Burchette JL, McLendon RE. CD34 and dural fibroblasts: the relationship to solitary fibrous tumor and meningioma. Acta Neuropathol. 2001;102(4):349–54.
22. Folpe AL, Billings SD, McKenney JK, Walsh SV, Nusrat A, Weiss SW. Expression of claudin-1, a recently described tight junction-associated protein, distinguishes soft tissue perineurioma from potential mimics. Am J Surg Pathol. 2002;26(12):1620–6.
23. Pina AR, Martinez MM, de Almeida OP. Glut-1, best immunohistochemical marker for perineurial cells. Head Neck Pathol. 2015;9(1):104–6. doi:10.1007/s12105-014-0544-6.
24. Hirose T, Tani T, Shimada T, Ishizawa K, Shimada S, Sano T. Immunohistochemical demonstration of EMA/Glut1-positive perineurial cells and CD34-positive fibroblastic cells in peripheral nerve sheath tumors. Mod Pathol. 2003;16(4):293–8. doi:10.1097/01.MP.0000062654.83617.B7.
25. van de Nes JA, Griewank KG, Schmid KW, Grabellus F. Immunocytochemical analysis of glucose transporter protein-1 (GLUT-1) in typical, brain invasive, atypical and anaplastic meningioma. Neuropathology. 2015;35(1):24–36. doi:10.1111/neup.12148.